THE JOURNAL OF IMMUNOLOGY

Guanylate Binding Protein 1–Mediated Interaction of T Cell Antigen Receptor Signaling with the Cytoskeleton

Florian Forster, Wolfgang Paster, Verena Supper, Philipp Schatzlmaier, Stefan Sunzenauer, Nicole Ostler, Anna Saliba, Paul Eckerstorfer, Nathalie Britzen-Laurent, Gerhard Schütz, Johannes A. Schmid, Gerhard J. Zlabinger, Elisabeth Naschberger, Michael Stürzl and Hannes Stockinger

J Immunol 2014; 192:771-781; Prepublished online 13 December 2013;
doi: 10.4049/jimmunol.1300377
http://www.jimmunol.org/content/192/2/771

The Journal of Immunology is published twice each month by
The American Association of Immunologists, Inc.,
9650 Rockville Pike, Bethesda, MD 20814-3994.

Print ISSN: 0022-1767 Online ISSN: 1550-6606.

Guanylate Binding Protein 1–Mediated Interaction of T Cell Antigen Receptor Signaling with the Cytoskeleton

Florian Forster,* Wolfgang Paster,* Verena Supper,* Philipp Schatzlmaier,* Stefan Sunzenauer,† Nicole Ostler,‡ Anna Saliba,* Paul Eckerstorfer,* Nathalie Britzen-Laurent,‡ Gerhard Schütz,† Johannes A. Schmid,§ Gerhard J. Zlabinger,¶ Elisabeth Naschberger,‡ Michael Stürzl,‡ and Hannes Stockinger*

GTPases act as important switches in many signaling events in cells. Although small and heterotrimeric G proteins are subjects of intensive studies, little is known about the large IFN-inducible GTPases. In this article, we show that the IFN-γ–inducible guanylate binding protein 1 (GBP-1) is a regulator of T cell activation. Silencing of GBP-1 leads to enhanced activation of early T cell Ag receptor/CD3 signaling molecules, including Lck, that is translated to higher IL-2 production. Mass spectrometry analyses showed that regulatory cytoskeletal proteins, like plastin-2 that bundles actin fibers and spectrin β-chain, brain 1 that links the plasma membrane to the actin cytoskeleton, are binding partners of GBP-1. The spectrin cytoskeleton influences cell spreading and surface expression of TCR/CD3 and the leukocyte phosphatase CD45. We found higher cell spreading and enhanced surface expression of TCR/CD3 and CD45 in GBP-1 silenced T cells that explain their enhanced TCR/CD3 signaling. We conclude that GBP-1 is a downstream processor of IFN-γ via which T cells regulate cytoskeleton-dependent cell functions.
***The Journal of Immunology*, 2014, 192: 771–781.**

Guanylate binding protein 1 (GBP-1) is a 67-kDa protein belonging to the family of IFN inducible GTPases, which itself belongs to the dynamin superfamily (1). GBP-1 expression is inducible through the T cell IFN-γ, but also via other inflammatory cytokines like TNF-α, IL-1β, and IL-1α (2, 3). Within the three-dimensional structure of GBP-1, an N-terminal globular domain can be distinguished from a C-terminal helical domain, which mediates an antiproliferative state in endothelial cells (2, 4). In the helical domain, a coiled-coil domain important for protein interactions and typical for structural or motor proteins is located (5). The C terminus contains an isoprenylation site for membrane binding.

Although the tertiary structure of GBP-1 has been solved, there is not much known about the physiologic role of GBP-1 (6, 7). GBP-1 inhibits the invasiveness and tube-forming capability of endothelial cells by inhibiting expression of matrix metalloproteinase-1 (8) and inducing integrin α4 expression (9). In addition, GBP-1 is an important player in cell-autonomous immunity (10). It was shown that loss of function of all GBP family members makes mice more susceptible to bacterial infection (11), most probably because GBPs interfere with autophagosomes. GBP-1 plays also a role in establishing an antiviral state against vesicular stomatitis virus and encephalomyocarditis virus in HeLa cells (12). Moreover, GBP-1 interferes with hepatitis C virus infection through interaction with the viral protein NS5B (13). The only cellular interaction partner of GBP-1 known so far is β-IIITubulin (14). This points to interaction of GBP-1 with structural proteins and suggests that overexpression of GBP-1 in paclitaxel-resistant cells is directly associated to the therapeutic failure of this antimitotic drug in certain tumors (15).

Although $CD4^+$ and $CD8^+$ T lymphocytes exhibit the highest relative GBP-1 expression in the human body (16), nothing is known about the function of GBP-1 in these cells. In contrast with GBP-1, there is already data available concerning p47 large GTPases and lymphocytes. In particular, Lrg-47 (also known as Ifi1, Irgm1) was found to be connected to IFN-γ–induced cell death and proliferation deficiencies in murine T cells (17). However, the collection of p47 GTPases in humans is limited to three genes, and none of those is induced by IFN-γ (18). The loss of IFN-γ–inducible p47 GTPases in humans warrants the speculation that their functions might be fulfilled by other proteins (19). Therefore, we asked whether GBP-1 could be one of those substitutes and which role it would play in adaptive immunity in humans.

In this study, we report human GBP-1 as a player in T cell activation interfering with the early stage of TCR signaling. We further discovered new cellular binding partners of GBP-1 and show that GBP-1 exerts its function in TCR signaling through interaction with structural proteins like plastin-2 and spectrin β-chain, brain 1 (βII-spectrin).

*Molecular Immunology Unit, Institute for Hygiene and Applied Immunology, Center for Pathophysiology, Infectiology and Immunology, Medical University of Vienna, 1090 Vienna, Austria; †Institute of Applied Physics, Vienna University of Technology, 1040 Vienna, Austria; ‡Division of Molecular and Experimental Surgery, University Medical Center Erlangen, Friedrich-Alexander University of Erlangen-Nuremberg, 91054 Erlangen, Germany; §Department of Vascular Biology, Center for Physiology and Pharmacology, Medical University of Vienna, 1090 Vienna, Austria; and ¶Institute of Immunology, Center for Pathophysiology, Infectiology and Immunology, Medical University of Vienna, 1090 Vienna, Austria

Received for publication February 8, 2013. Accepted for publication November 12, 2013.

This work was supported by the GEN-AU program of the Austrian Federal Ministry for Science and Research, the German Research Foundation (DFG; Grants STU 317/2-1 and STU 238/6-1 to M.S.), the German Cancer Aid (Grant 109510 to M.S.), and a DOC fellowship of the Austrian Academy of Sciences (to S.S.).

Address correspondence and reprint requests to Dr. Hannes Stockinger, Medical University of Vienna, Lazarettgasse 19, 1090 Vienna, Austria. E-mail address: hannes.stockinger@meduniwien.ac.at

The online version of this article contains supplemental material.

Abbreviations used in this article: eEF1-a, eukaryotic translation elongation factor 1A; GBP-1, guanylate binding protein 1; MRCL3, myosin regulatory L chain MRCL3 variant; SEE, staphylococcus enterotoxin E; shCtrl, sh control; shRNA, short hairpin RNA; SILAC, stable isotope labeling by amino acids in cell culture; βII-spectrin, spectrin β-chain, brain 1; STOML2, stomatin-like protein 2.

Materials and Methods

Plasmids, oligonucleotides, and Abs

GFP-tagged GBP-1 (generated in the Erlangen laboratory) was cloned into the retroviral vector pBMN-Z (provided by G. Nolan, Stanford University School of Medicine, Stanford, CA). P-tagged GBP-1 was cloned into the retroviral vector pBMN-IRES-GFP. Empty pBMN-IRES-GFP vector was used as vector control. The short hairpin RNA (shRNA) expression vector pLKOpuro1 (provided by S. Stewart, Washington University School of Medicine, St. Louis, MO) was used to express control and GBP-1–specific shRNA. For the expression of plastin-2 shRNA, the retroviral shRNA expression vector pSM2c (Open Biosystems, Huntsville, AL) was used. The following sequences were used for shRNA-mediated knockdown of gene expression: shGBPp1 sense strand at position 1467: 5′-CCGGT*TGAAGTGGAACGTGTGAAA*TTCAAGAGA*TTTCACACGT-TCCACTTCA*TTTTTG-3′; shGBPp2 sense strand at position 492: 5′-CCG-GT*GGTTGAGGATTCAGCTGAC*TTCAAGAGA*GTCAGCTGAATCCTCAA-CC*TTTTTG-3′; shPlastinp1 sense strand at position 1714: 5′- TGCTGTT-GACAGTGAGCG*CGGCCTTGATTTGGCAGCTAAT*TAGTGAAGCCACA-GATGT*AATTAGCTGCCAAATCAAGGCCA*TGCCTACTGCCTCGGA-3′; shPlastinp2 sense strand at position 2260: 5′- TGCTGTTGACAGTG-AGCG*ACCAAGTAGCCTCTCCTGTATT*TAGTGAAGCCACAGATGTA-*AATACAGGAGAGGCTACTTGGC*TGCCTACTGCCTCGGA-3′. Gene-specific shRNA target sequences are indicated in italic. For silencing of βII-spectrin, we purchased two shRNAs from Sigma-Aldrich with the TRC numbers TRCN0000116822 (shSpectrin1) and TRCN0000296592 (shSpectrin2), respectively. As sh control (shCtrl), we used the MISSION Non-Target pLKOpuro1 control vector (Sigma-Aldrich).

The helper plasmids used for lentiviral expression vectors were psPAX2 and pMD2.G (constructed by D. Trono, Ecole Polytechnique Federal de Lausanne; obtained via Addgene, Cambridge, MA) and for retroviral expression vectors pGagPol (Addgene) and pMD2.G. The following primers were used for quantitative RT-PCR: GBP-1 forward: 5′-GGTCCAGTTGCTGAAAGAGC-3′; GBP-1 reverse: 5′-CTTGGTTAGGGGTGACAGGA-3′. For normalization, the following primers of eukaryotic translation elongation factor 1A (eEF1-a) were used: EEF1-a forward: 5′-GTGCTAACATGCCTTGGTTC-3′; EEF1-a reverse: 5′-AGAACACCAGTCTCCACTCG-3′. Rat anti–GBP-1 mAb (clone 1B1) was generated in the Erlangen laboratory. Rabbit anti-actin Ab was obtained from Sigma-Aldrich; CD3 mAb MEM-57, anti–p-tag mAb H902, CD59 mAb MEM-43, CD43 mAb MEM-59, and CD147 mAb MEM-M6/1 were kind gifts from V. Horejsi (Institute of Molecular Genetics, Academy of Sciences of the Czech Republic, Prague, Czech Republic). CD147 mAb MEM-M6/1 was directly conjugated with AF647 succinimidyl ester (Life Technologies, Carlsbad, CA) in our laboratory. Rabbit anti-histone H3.1 Ab was purchased from Signalway Ab (College Park, MD). Rabbit anti-Zap70 (99F2) mAb, rabbit anti–phospho-Y416-Src Ab, rabbit anti–phospho-Y505-Lck Ab, rabbit anti–phospho–Y783–PLC-γ Ab, rabbit anti–phospho-T202/Y204-p44/p42 (D13.14.4E) mAb, rabbit anti–α/β-tubulin Ab, the calnexin-specific mAb (C5C9), and rabbit anti–plastin-2 Ab were purchased from Cell Signaling Technologies (Beverly, MA). Anti-TCR β-chain mAb C305 was kindly provided by A. Weiss (University of California, San Francisco, CA). The mAb OKT3 to CD3 was obtained from Ortho Pharmaceuticals (Raritan, NJ). mAb Leu^{28} to CD28, phospho-Y319-Zap-70 pAb, and phospho-Y142-CD3ζ (K25-407.69) mAbs were purchased from BD Biosciences (Franklin Lakes, NJ). Anti–plastin-2 mAb LPL4A.1 and the rabbit pAb against βII-spectrin were purchased from Abcam (Cambridge, MA). Allophycocyanin-conjugated CD4 mAb MEM-241 and Pacific orange–conjugated CD45 mAb FN50 were from EXBIO (Prague, Czech Republic). Pacific blue–conjugated mouse anti-human CD69 mAb (FN50) was purchased from Biolegend (San Diego, CA). Goat anti-mouse IgG (H + L) Ab coupled to AF555 was purchased from Invitrogen (Grand Island, NY), anti-phosphotyrosine (p-Tyr) mAb 4G10 and rabbit anti-human linker for activation of T cells (LAT) Ab from Millipore (Billerica, MA), rabbit anti–phospho-Y191-LAT Ab from Biosource/Invitrogen (Grand Island, NY), and rabbit anti-human Lck mAb

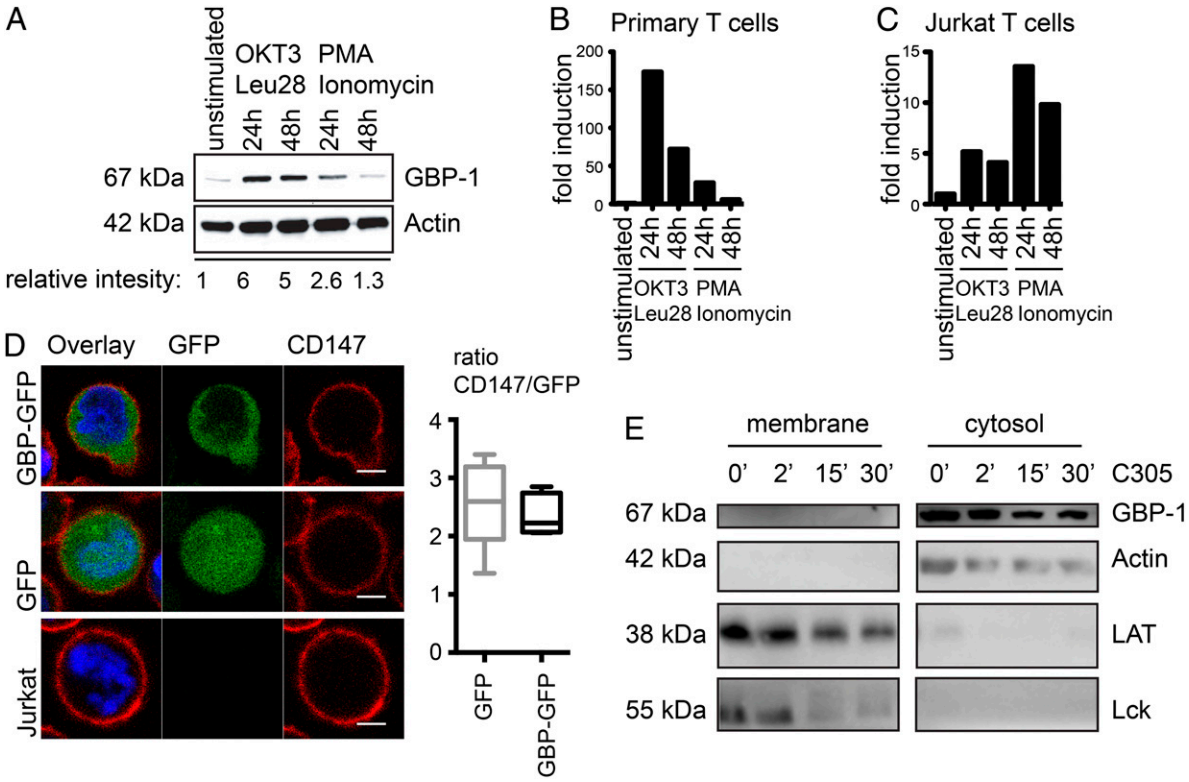

FIGURE 1. GBP-1 expression and localization upon T cell stimulation. (**A**) Immunoblotting analysis of GBP-1 in samples of unstimulated and OKT3/Leu^{28}- or PMA/ionomycin-stimulated human peripheral blood T lymphocytes. Numbers indicate relative expression of GBP-1 normalized to actin expression in comparison with unstimulated cells. (**B**) mRNA expression of GBP-1 in human peripheral blood T lymphocytes. (**C**) mRNA expression of GBP-1 in Jurkat T cells. (B and C) GBP-1 mRNA expression levels were normalized to eEF1 mRNA expression levels. (**D**) A representative confocal fluorescence image of Jurkat T cells expressing GFP-tagged GBP-1 or naked GFP. The plasma membrane was stained using CD147 mAb MEM-M6/1. The diagram on the right shows the ratio of the fluorescence intensity between CD147 and GFP at the cell membrane estimated by the ImageJ macro EdgeRatio. $n = 10$ for Jurkat T cells expressing GFP or GBP-1–GFP. Scale bars, 5 μm. (**E**) Immunoblot of membrane and cytosolic fractions of Jurkat T cells stimulated with the TCR β-chain mAb C305 for indicated time points. Actin and LAT served as marker for the cytosolic and the membrane fraction, respectively. The appearance of the 59-kDa band in the immunoblot of Lck proved activation of the cells. One representative experiment of at least three independent experiments is shown in each panel.

H95 from Santa Cruz (Santa Cruz, CA). Peroxidase-conjugated goat anti-rat IgG (H + L) Ab was bought from Dianova (Hamburg, Germany). Goat anti-rabbit IgG (H + L) and rabbit anti-mouse IgG (whole-molecule) Abs, both HRP conjugated, were from Bio-Rad (Hercules, CA) and Sigma-Aldrich, respectively. Goat anti-mouse IgG + IgM (H + L) Ab conjugated with allophycocyanin and goat anti-mouse IgG + IgM (H + L) $F(ab')_2$ were obtained from Jackson Immunoresearch (West Grove, PA); FITC-conjugated sheep anti-mouse IgG + IgM $F(ab')_2$ was kindly provided by An der Grub (Kaumberg, Austria).

Cells

The T cell line Jurkat E6.1, human PBMCs, B cell line Raji, and HEK293T cells were maintained in RPMI 1640 or DMEM medium supplemented with 100 μg/ml penicillin, 100 μg/ml streptomycin, 2 mM L-glutamine (all from Invitrogen), and 10% heat-inactivated FCS (Sigma-Aldrich). All cells were grown in a humidified atmosphere at 37°C and 5% CO_2, and split every 2–3 d to maintain viability.

Immunoblotting

Cells (2×10^7 / ml) were lysed for 25 min at 4°C in ice-cold lysis buffer (20 mM Tris-HCl [pH 7.5], 150 mM NaCl, 2 mM EDTA [all from Roth], and complete protease inhibitor tablets [Roche, Basel, Switzerland]) containing 1% detergent Nonidet P-40 (Thermo Scientific, Waltham, MA). The insoluble material was removed by centrifugation at 10,000 × *g* for 2 min at 4°C, and the supernatant was subjected to standard SDS-PAGE gel electrophoresis (Peqlab, Erlangen, Germany) followed by semidry Western blotting. The blots were developed using HRP substrate (Biozym, Hessisch Oldendorf, Germany) and monitoring light emission in a Fuji LAS-4000 imager (Fuji, Tokyo, Japan). Signals were quantified using ImageJ software.

Quantitative RT-PCR

After stimulation of cells with OKT3 (1 μg/ml) and Leu^{28} (0.5 μg/ml) or with 10 ng/ml PMA plus 100 ng/ml ionomycin, cDNA was synthesized with the Superscript II first-strand synthesis system of the RT-PCR kit (Invitrogen) using 1 μg TRI-reagent (Sigma) extracted RNA and poly-dT primers supplied with the kit, according to the manufacturer's protocol. PCR was carried out in a LightCycler instrument with the LightCycler FastStart DNA master SYBR green I kit (all Roche) according to the manufacturer's protocol.

Cell fractionation

Membrane, cytosolic/cytoskeletal, and nuclear fractions were isolated from cells as described elsewhere (20) and subjected to Western blot analysis.

Transduction of Jurkat T cells and PBMCs

Transduction of Jurkat T cells and PBMCs was performed as previously described (21).

Confocal fluorescence microscopy

Jurkat T cells expressing either GFP-tagged GBP-1 or GFP alone were allowed to adhere on poly-L-lysine–coated adhesion slides for 10 min (Marienfeld, Lauda-Königshofen, Germany). Cells were fixed with 4% paraformaldehyde (Merck, Whitehouse Station, NJ) in PBS for 5 min followed by permeabilization for 10 min with 0.1% Triton X-100 (Thermo Scientific, Waltham, MA). For labeling of the Jurkat T cell membrane AF647-conjugated CD147 mAb, MEM-M6/1 was used. Slides were mounted with Vectashield Mounting Medium with DAPI (Vector Laboratories, Burlingame, CA). Cells were analyzed on a confocal Zeiss LSM 700 microscope (Carl Zeiss Ag, Oberkochen, Germany), equipped with a "Plan-Apochromat" 63×/1.40 Oil DIC M27 objective. Pictures were acquired with the ZEN 2009 software. The distribution of the GFP signal was evaluated using the ImageJ macro EdgeRatio (http://cail.cn/programming.html). The ratio of the mean intensity values of the CD147 staining versus the GFP signal was calculated for the region of the cell exhibiting the highest CD147 signal.

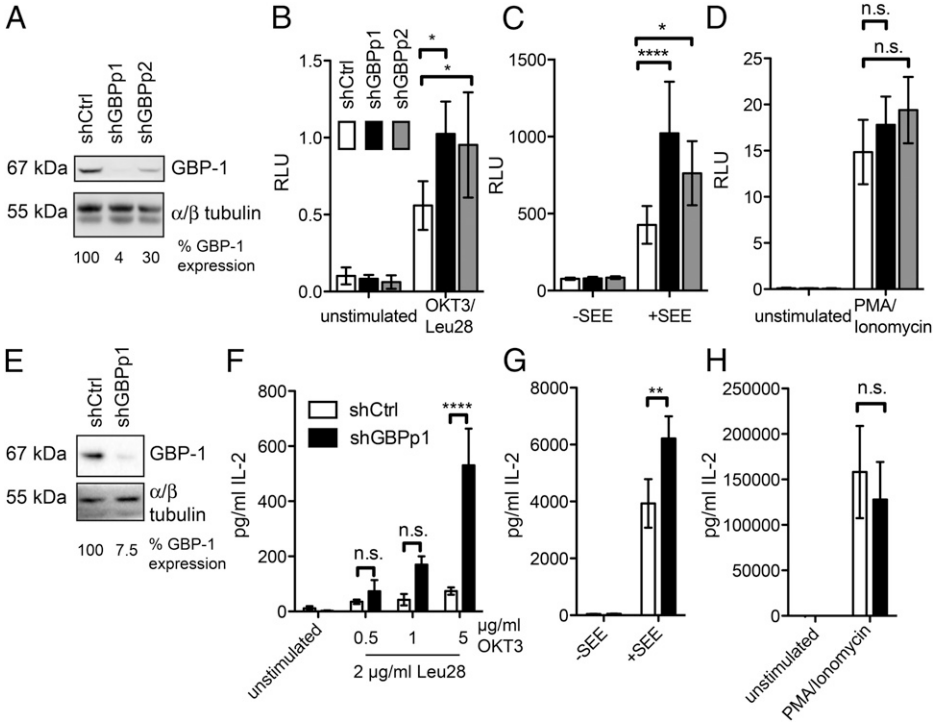

FIGURE 2. Silencing of GBP-1 leads to higher IL-2 expression in T cells. (**A**) Immunoblot of Jurkat T cells transduced with a control shRNA or two different shRNAs targeting GBP-1 at two different positions. GBP-1 expression was normalized to tubulin. (**B**) Relative light units of Jurkat cells stably transfected with an IL-2 luciferase reporter and silenced for GBP-1 with the two different GBP-1–specific shRNAs. Jurkat T cells were either left unstimulated or were stimulated with OKT3/Leu-28. (**C**) The cells in (B) were stimulated with staphylococcus enterotoxin E (SEE)–pulsed Raji B cells. (**D**) The cells in (B) were stimulated with PMA/ionomycin. (**E**) Immunoblot of GBP-1 upon silencing in human peripheral blood T lymphocytes. GBP-1 expression was normalized to tubulin. (**F**) IL-2 concentrations in the supernatants of control and GBP-1–silenced peripheral blood T lymphocytes stimulated with the indicated concentrations of OKT3/Leu^{28}. (**G**) IL-2 concentrations in the supernatants of control and GBP-1–silenced T lymphocytes stimulated with Raji B cells pulsed with or without SEE. (**H**) IL-2 concentrations in the supernatants of control and GBP-1–silenced T lymphocytes stimulated with PMA/ionomycin. (B–D) Bars represent the mean of at least three independent experiments; error bars represent SEM. (F–H) Bars indicate the mean; error bars represent SD of a representative experiment of at least three different ones. $*p < 0.05$, $**p < 0.01$, $****p < 0.001$.

Luciferase reporter gene assay

Jurkat T cells stably expressing an IL2-luciferase reporter were stimulated with either 1 μg/ml OKT3/0.5 μg/ml Leu^{28}, or Raji B cells pulsed with 10 ng/ml staphylococcus enterotoxin E (SEE) or 10 ng/ml PMA plus 100 ng/ml ionomycin. Luciferase assays were performed using the luciferase reporter gene assay kit (Roche) according to the manufacturer's instructions. Relative luminescence was measured either in the Mithras LB 940 multimode plate reader (Berthold Technologies, Bad Wildbach, Germany) or, for Fig. 2B and 2D, in a Lumat LB 9501 device (Berthold Technologies) and normalized for protein content with the Bio-Rad protein assay (Bio-Rad, Hercules, CA).

Measurement of secreted IL-2

Samples were analyzed using the Luminex xMAP suspension array technology (Multimetrix, Heidelberg, Germany). Thirty microliters of cell culture supernatants was used. Standard curves were generated using rIL-2 (R&D Systems, Minneapolis, MN).

Thymidine incorporation assay

Cells were seeded in a 96-well flat-bottom plate in 200 μl RPMI 1640 medium supplemented with 1 μCi [^{3}H]thymidine. After stimulation for 18 h with 1 μg/ml OKT3 and 0.5 μg/ml Leu^{28}, the cells were broken up by a freeze/thaw cycle and harvested on a cell harvester (Tomtec, Hamden, CT). Filters were analyzed in a scintillation counter (Wallac).

Stable isotope labeling by amino acids in cell culture labeling

Jurkat T cells were cultured in RPMI 1640 medium (lacking arginine and lysine; Invitrogen), 10% FCS, and supplemented either with the heavy (R6K4) or light (R0K0) forms of L-arginine and L-lysine. Labeling efficiency was tested by liquid chromatography–tandem mass spectrometry after 10 d, and at that time the general labeling incorporation was already >98% for all identified proteins.

Protein extraction and phospho-peptide enrichment

Cells were lysed in 4% SDS (Roth), 0.1 M Tris-HCl (pH 7.6) with protease and phosphatase inhibitors (Roche). Protein contents were estimated by fluorimetric tryptophan measurement. Equal protein amounts from control or GBP-1–silenced cells were pooled, reduced with 0.1 M DTT (Roth), digested with trypsin and lysC, and rebuffered by filter-aided sample preparation as described previously (22). Sequential phosphopeptide isolation with TiO_2 beads (MZ-Analysentechnik, Mainz, Germany) was done as described previously (23).

Immunoprecipitation

Cells were lysed in ice-cold lysis buffer (20 mM Tris-HCl [pH 7.5], 150 mM NaCl, and complete protease inhibitor tablets) containing 1% detergent Brij58 (Thermo Scientific). After removing insoluble material, the supernatant was mixed with 50 μl Sepharose beads (GE Healthcare, Little Chalfont, U.K.) coupled to the p-tag specific mAb H902. After an incubation for 1 h at 4˚C with constant rotation, the beads were washed three times with lysis buffer and elution was performed using 1.5× Laemmli buffer. For mass spectrometry analysis, elution was performed with 6 M urea, 2 M thiourea (Sigma-Aldrich) in 10 mM HEPES, pH 8.0 (Biomol GmbH, Hamburg, Germany), and the resulting sample was trypsin (Promega, Fitchburg, WI) and LysC (WAKO, Osaka, Japan) digested overnight. For the precipitation of endogenous GBP-1, beads covalently crosslinked with GBP-1 mAb 1B1 by BS3 (Thermo Fisher Scientific) were used.

Analysis of protein phosphorylation

Cells were rested in RPMI 1640 medium supplemented with 1% FCS for 1 h at 37˚C. Jurkat T cells (1.5×10^6 cells/time point) were stimulated for different time points at 37˚C using a 1:100 dilution of the hybridoma supernatant of the TCR mAb C305. Peripheral blood T lymphocytes (3×10^6 cells/time point) were stimulated with 10 μg/ml CD3 mAb OKT3

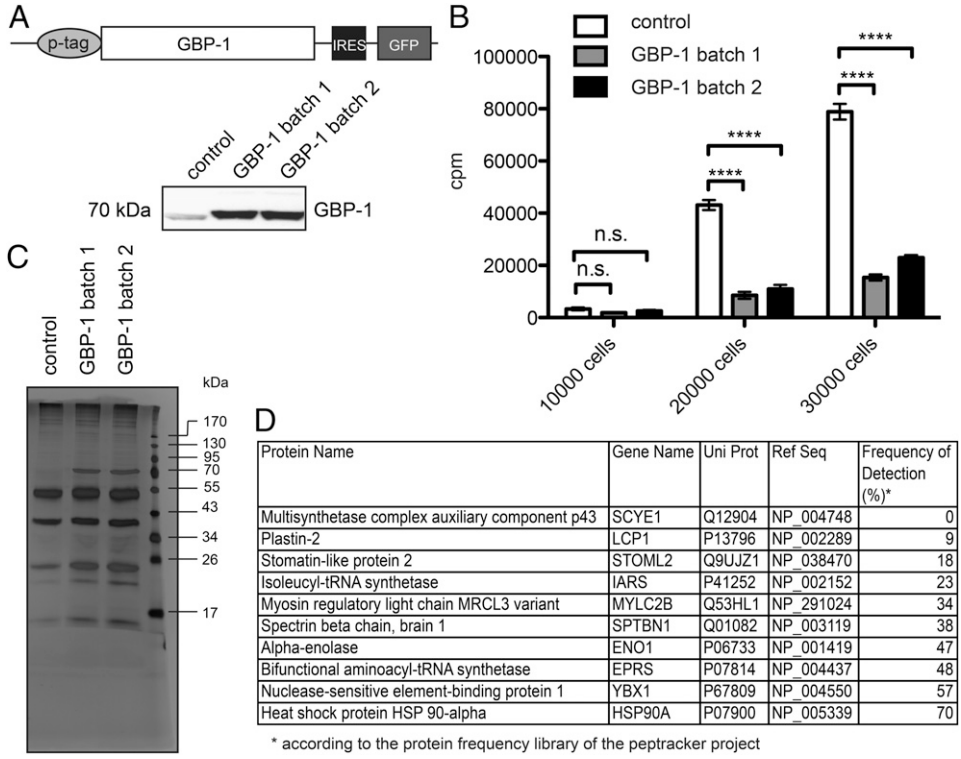

D

Protein Name	Gene Name	Uni Prot	Ref Seq	Frequency of Detection (%)*
Multisynthetase complex auxiliary component p43	SCYE1	Q12904	NP_004748	0
Plastin-2	LCP1	P13796	NP_002289	9
Stomatin-like protein 2	STOML2	Q9UJZ1	NP_038470	18
Isoleucyl-tRNA synthetase	IARS	P41252	NP_002152	23
Myosin regulatory light chain MRCL3 variant	MYLC2B	Q53HL1	NP_291024	34
Spectrin beta chain, brain 1	SPTBN1	Q01082	NP_003119	38
Alpha-enolase	ENO1	P06733	NP_001419	47
Bifunctional aminoacyl-tRNA synthetase	EPRS	P07814	NP_004437	48
Nuclease-sensitive element-binding protein 1	YBX1	P67809	NP_004550	57
Heat shock protein HSP 90-alpha	HSP90A	P07900	NP_005339	70

* according to the protein frequency library of the peptracker project

FIGURE 3. Binding partners of GBP-1 identified by mass spectrometry. (**A**) (*Top panel*) Scheme of p-tagged GBP-1 used for overexpression. (*Bottom panel*) Two batches of the Jurkat T cell clone E6.1 were transduced with p-tagged GBP1-IRES-GFP, sorted for GFP expression followed by expression analysis of p-tagged GBP-1 by immunoblotting. (**B**) The cells in (A) were analyzed for proliferation by thymidine incorporation. The cpms are shown for the indicated cell numbers stimulated with OKT3/Leu^{28} for 18 h. One representative experiment of three is shown. Bars represent mean and error bars SD. ****$p < 0.001$. (**C**) Silver staining analysis of the precipitates from the two p-tagged GBP-1–expressing Jurkat batches in (A). The immunosorbent was anti–p-tag mAb H902 directly coupled to cyanogen bromide–activated Sepharose beads. Lysates of Jurkat T cells not expressing p-tagged GBP-1 were used for control precipitation. (**D**) Proteins identified by mass spectrometry. The proteins displayed showed a positive intensity after subtraction of the negative control in four independent mass spectrometry runs. The identified proteins were sorted according to their frequency of detection estimated by the protein frequency library of the PepTracker project (51). Proteins with high frequency reflect a certain degree of unspecificity.

cross-linked with 5 μg/ml goat anti-mouse IgG + IgM (H + L) $F(ab')_2$. The reactions were stopped by the addition of ice-cold washing buffer (20 mM Tris-HCl [pH 7.5], 150 mM NaCl, and 5 mM EDTA). After centrifugation (2 min at 850 × *g* and 4°C), cells were immediately lysed and subjected to immunoblotting as described previously. The lysis buffer was supplemented with 1 mM sodium orthovanadate (Sigma-Aldrich) and 20 mM NaF (Sigma-Aldrich).

Flow cytometry

Cells were washed with staining buffer [1% BSA (Roth) and 0.02% NaN_3 (Sigma-Aldrich) in PBS], and incubated for 30 min with 4 μg/ml human Ig (CSL Behring, King of Prussia, PA) on ice. Primary Ab (10 μg/ml) was added and the cells were incubated for 30 min on ice. Cells were washed with staining buffer and, if needed, incubated with conjugated secondary Ab (10 μg/ml) for 30 min on ice. After a final wash, cells were analyzed on an LSRII flow cytometer (BD Biosciences).

Peptide separation and mass spectrometry

The peptides were desalted by RPC18 StageTip columns (Agilent Technologies, Santa Clara, CA) and loaded on Spare part Agilent NanoHPLC (Agilent Technologies) filled with reversed-phase ReproSil-Pur C18-AQ 3 μm resin (Dr. Maisch GmbH, Ammerbuch-Entringen, Germany). The sample was eluted with a gradient ranging from 2 to 40% MeCN (Merck) in 0.5% acetic acid (Roth) over 100 min and a flow rate of 250 nL/min. The eluate was analyzed with an LTQ Orbitrap mass spectrometer (Thermo Electron, Bremen, Germany). Results were evaluated with Max Quant software (24) and Andromeda database search engine (25), and label-free quantification algorithm (26) was used to make several independent experiments comparable.

Cell spreading assay

Epoxy-functionalized glass coverslips were provided by CBL GmbH (Linz, Austria). Silicon incubation chambers (Secure-Seal hybridization chambers; Sigma-Aldrich) were stuck onto the slides and filled with 1 μg/ml OKT3 mAb and 0.5 μg/ml Leu-28 mAb in PBS for 1 h. Cells were stained using an AF647-labeled CD59 mAb, and time-lapse imaging was started directly after the cells were seeded on the mAb-coated slides. The imaging was done on a system based on a Zeiss Axiovert 200/M microscope equipped with a Zeiss α-Fluar 100× objective (NA = 1.45) under total internal reflection settings. Scanning was performed in time delay and integration mode. (For further details concerning the setup, see Ref. 27.) Cell spreading of individual cells was assessed using the ImageJ software.

Calcium flux measurement

Calcium flux measurements were performed as described previously (28).

Statistical analysis

If not stated otherwise, unpaired Student *t* test or two-way ANOVA followed by Bonferroni posttest was performed using GraphPad Prism (GraphPad Software, San Diego, CA).

Results

GBP-1 is upregulated upon T lymphocyte activation and located in the cytosol of T cells

Basal GBP-1 expression in human peripheral blood T lymphocytes can be increased by stimulation with mAbs to CD3 (OKT3) plus CD28 (Leu^{28}) or PMA plus ionomycin (Fig. 1A). This was due to higher GBP-1 transcription demonstrated by quantitative RT-PCR in primary T lymphocytes, as well as in Jurkat T cells (Fig. 1B, 1C). Because GBP-1 possesses an isoprenylation site for possible membrane binding, we monitored the localization of GBP-1. We therefore transduced Jurkat T cells with either GFP-tagged GBP-1 or GFP alone as a control. After transduction, the cells were sorted for high and equal levels of GFP expression and immunostained for CD147 as a surface marker. Colocalization analysis with CD147 showed that GFP–GBP-1 and control protein GFP were exclusively expressed in the cytosol of Jurkat T cells (Fig. 1D). Cell fractionation experiments confirmed the cytosolic localization of GBP-1, and stimulation of Jurkat T cells with the TCR β-chain mAb C305 for different time points did not lead to membrane binding of GBP-1 (Fig. 1E, Supplemental Fig. 1).

GBP-1 regulates IL-2 expression in T cells

To evaluate a functional role for GBP-1 in T cells, we silenced GBP-1 expression using two different lentiviral delivered shRNA constructs (Fig. 2A). Silencing of GBP-1 with both shRNAs in Jurkat T cells expressing an IL-2 promoter–driven luciferase reporter gene resulted in higher IL-2 promoter activity after stimulation with CD3 and CD28 mAbs or SEE pulsed Raji B cells

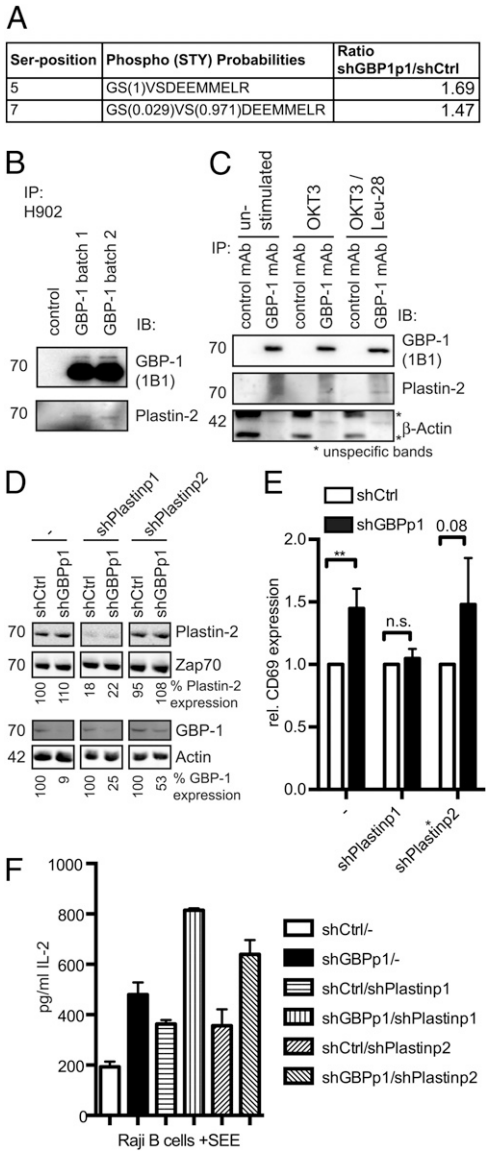

FIGURE 4. GBP-1 interaction with plastin-2. (**A**) The ratio of plastin-2 phosphorylation of control silenced to GBP-1–silenced cells estimated by SILAC and mass spectrometry. (**B**) Coimmunoprecipitation of p-tagged GBP-1 and plastin-2 in Jurkat T cells. (**C**) Coimmunoprecipitation of endogenous GBP-1 with plastin-2 and β-actin from lysates of peripheral human T lymphocytes. (**D**) Immunoblotting analysis of lysates of Jurkat T cells transduced with GBP-1 shRNA alone or in combination with shRNAs specific for plastin-2. (**E**) CD69 expression on the surface of Jurkat T cells. The cells were silenced for GBP-1 alone or in combination with the functional shRNA for plastin-2 (shPlastinp1), or with the nonfunctional shRNA shPlastinp2. The cells were stimulated for 14 h with OKT3/Leu^{28}–coated beads. Values were normalized to CD69 expression in Jurkat T cells transduced with control shRNA. $^{**}p < 0.01$. (**F**) IL-2 concentrations in the supernatants of the cells in (D) stimulated for 7 h with Raji B cells pulsed with SEE. (E and F) Bars represent the mean; error bars represent SD of at least three independent experiments.

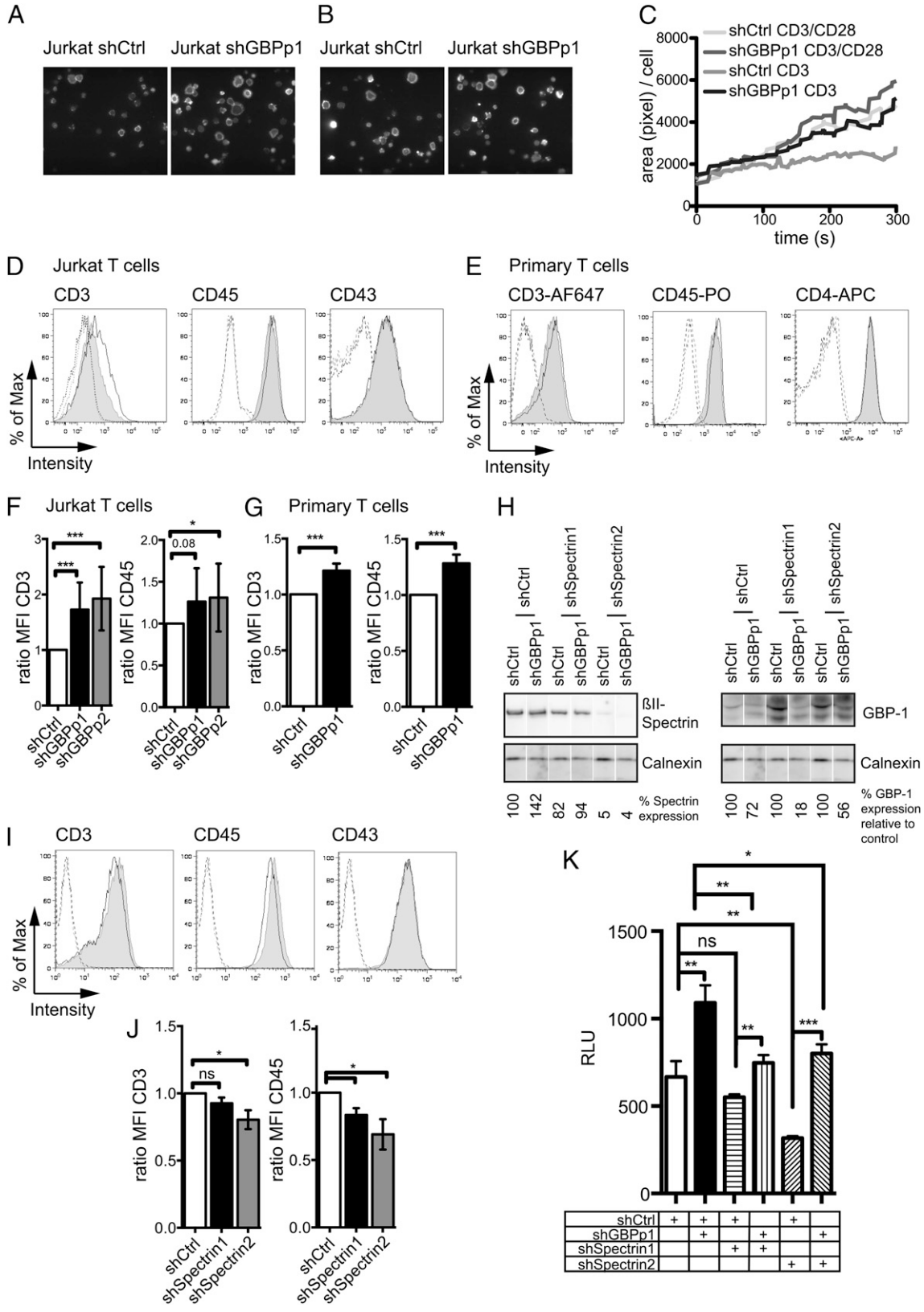

FIGURE 5. Influence of GBP-1 on T cell spreading and surface expression of CD3 and CD45. (**A**) Spreading of Jurkat T cells transduced with GBP-1 or control shRNA for 5 min on a glass slide coated with OKT3 mAb. (**B**) Spreading of the same cells for 5 min on a glass slide coated with OKT3 and Leu^{28} mAbs. (**C**) Spreading area over time of individual Jurkat T cells on the coated surfaces. The following numbers of cells were evaluated: shGBP1p1 on the OKT3 surface: $n = 58$; shCtrl on the OKT3 surface: $n = 60$; shGBP1p1 on the OKT3/Leu^{28} surface: $n = 29$; and shCtrl on the OKT3/Leu-28 surface: $n = 32$. For better visualization, the smoothing of mean spreading area/cell is shown. For this figure with error bars, see Supplemental Fig. 3. (**D**) Representative flow cytometric analysis of the indicated markers on the surface of GBP-1–silenced or control silenced Jurkat T cells. (**E**) Representative flow cytometric analysis of the indicated markers on the surface of GBP-1–silenced or control silenced primary T lymphocytes. (**F**) Statistical evaluation of the mean fluorescence intensity (MFI) ratio of CD3 and CD45 in GBP-1–silenced or control silenced Jurkat cells. (**G**) Statistical evaluation of the MFI ratio of CD3 (*Figure legend continues*)

compared with cells transduced with a control shRNA (Fig. 2B, 2C). In contrast, bypassing early TCR signaling by stimulation of these cells with PMA/ionomycin did not lead to higher IL-2 expression (Fig. 2D). Enhanced IL-2 promoter activity in GBP-1–silenced cells was independent of the time used for stimulation (Supplemental Fig. 2A). We verified our promoter studies by detecting higher IL-2 protein concentrations in the supernatant of GBP-1–silenced Jurkat T cells irrespective of the SEE concentration used (Supplemental Fig. 2B). We further verified our results with primary human peripheral blood T lymphocytes. GBP-1 expression was efficiently silenced with shRNA construct 1 (Fig. 2E). GBP-1–silenced T lymphocytes stimulated with increasing concentrations of CD3/CD28 mAbs or SEE-pulsed Raji B cells showed higher IL-2 concentrations in the culture supernatants (Fig. 2F, 2G). Again, no difference was observed when we used PMA/ionomycin for stimulation (Fig. 2H).

Identification of interaction partners of GBP-1

To identify interaction partners, which may explain the effects of GBP-1 on T cell activation, we stably overexpressed GBP-1 in Jurkat T cells. We used a p-tagged GBP-1 in a retroviral pBMN-IRES-GFP expression system. Independent transduction and sorting for high GFP expression led to the generation of two batches of p-tagged GBP-1–expressing Jurkat T cells (Fig. 3A). Both GBP-1–overexpressing cell batches showed reduced proliferation upon stimulation with CD3/CD28 mAbs (Fig. 3B). This is in accordance with results obtained with endothelial cells (6). We used these cell lines to precipitate GBP-1 with a p-tag–specific mAb (clone H902). The precipitate was analyzed by silver stain and GBP-1–specific immunoblotting to estimate precipitation efficiency of GBP-1 and to ensure adequate purity for subsequent mass spectrometry (Figs. 3C, 4B). As a negative control, we used cell lysates derived from Jurkat cells not expressing p-tagged GBP-1. For each mass spectrometry run, the intensities of the precipitated proteins in the negative control were subtracted from the intensities obtained with the p-tag–specific immunoprecipitation. To increase confidence of identification, we analyzed four independent mass spectrometry runs from the two GBP-1–overexpressing Jurkat T cell batches. We judged as potential binding partners of GBP-1 those molecules that were present in each of the four independent experiments. Based on this criterion, 10 proteins were classified as interaction partners of GBP-1 (Fig. 3D).

Influence of GBP-1 on and interaction with plastin-2

With the help of stable isotope labeling by amino acids in cell culture (SILAC)–based mass spectrometry, it is possible to identify quantitative differences in the phosphorylation status of a protein in distinct populations of cells. For this purpose, GBP-1–silenced Jurkat T cells were grown in culture medium containing the light forms of L-arginine and L-lysine, whereas wild type Jurkat cells were grown in culture medium supplemented with the heavy forms of L-arginine and L-lysine. The two populations were combined before sequential phospho-peptide enrichment and liquid chromatography–tandem mass spectrometry analysis. Using this technique, we identified two altered phosphorylation sites in plastin-2, 1 of the 10 potential interaction partners identified previously: serine residues 5 and 7, known to play a role in actin bundling (29) and T cell regulation (30), were constitutively higher phosphorylated in GBP-1–silenced Jurkat T cells (Fig. 4A). To corroborate the mass spectrometry data, we performed coimmunoprecipitation experiments with the Jurkat T cell batches overexpressing p-tagged GBP-1. As shown in Fig. 4B, we were able to coimmunoprecipitate plastin-2 with p-tagged GBP-1. To exclude possible effects of the p-tag or cell line artifacts, we precipitated endogenous GBP-1 of Jurkat T cells and of primary T lymphocytes, left either unstimulated or stimulated with OKT3 alone or in combination with Leu^{28} for 24 h. Again, we obtained coimmunoprecipitation of GBP-1 and plastin-2 (Fig. 4C). Because plastin-2 controls the assembly of the actin cytoskeleton into bundles (29), we were interested whether GBP-1 was capable of associating with β-actin. Indeed, we found β-actin as a binding partner of GBP-1 in three of the four mass spectrometry runs performed. Further, we coprecipitated endogenous GBP-1 and β-actin from lysates of primary human T lymphocytes (Fig. 4C).

To analyze whether plastin-2 plays a role in the phenotype of shGBP-1 cells, we used Jurkat T cells doubly silenced for GBP-1 and plastin-2. For plastin-2 silencing, we used two retrovirally delivered shRNAs specific for two different positions in the plastin-2 mRNA. The plastin-2 shRNA shPlastinp1 yielded a silencing efficiency of around 80%. The second position, shPlastinp2, did not show a reduction of plastin-2 expression. Therefore, we used the latter construct as a control shRNA for plastin-2 silencing (Fig. 4D). Wabnitz et al. (30) reported that higher plastin-2 activation led to a higher CD69 surface display in T cells that was dependent on the transport of CD69 to the surface. Strikingly, we were able to blunt the higher CD69 expression in GBP-1–silenced Jurkat T cells by cosilencing of plastin-2 (Fig. 4E). In addition, we assessed the IL-2 protein concentration in the supernatants of singly and doubly silenced cells stimulated with SEE pulsed Raji B cells (Fig. 4F). Cosilencing of GBP-1 and plastin-2 did not alter the higher IL-2 expression observed in Jurkat T cells silenced for GBP-1 alone. Moreover, silencing of plastin-2 did not abrogate IL-2 expression in human cells.

In summary, although this set of experiments shows a physical and functional interaction between GBP-1 and plastin-2 in terms of CD69 expression, this interaction is not responsible for the enhanced IL-2 expression upon TCR/CD3 stimulation of GBP-1–silenced T cells. So the question remained which interaction partner of GBP-1 transduced IL-2 inhibitory signals during T cell activation.

Influence of GBP-1 on cell spreading and expression of CD3 and CD45

Because the actin cytoskeleton is essential to drive T cell spreading to organize the immunological synapse (31), we aimed to prove whether the cytoskeleton contributed to higher activation of

and CD45 in GBP-1–silenced or control silenced primary T cells. (**H**) Immunoblotting analysis of lysates of Jurkat T cells transduced with GBP-1–silenced or control shRNA alone or in combination with shRNAs specific for βII-spectrin. (**I**) Flow cytometry analyses of the indicated markers on the surface of βII-spectrin or control silenced Jurkat T cells. (**J**) Statistical evaluation of the MFI ratio of CD3 and CD45 in βII-spectrin–silenced or control silenced Jurkat T cells. (**K**) Relative light units of Jurkat T cells stably transfected with an IL-2 luciferase reporter and cosilenced for GBP-1 and the two different βII-spectrin–specific shRNAs. The cells were stimulated for 7 h with SEE-pulsed Raji B cells. (F, G, J, and K) Bars represent the mean; error bars represent SD of at least three independent experiments. (F, G, and J) A paired *t* test was used to calculate significance. (D, E, and I) Gray area indicates the fluorescence intensity (FI) of the specific staining in control silenced cells. Black line specifies the FI of the specific staining in GBP-1– or βII-spectrin–silenced cells, respectively. Dashed gray lines show FI of the isotype control Ab in shCtrl cells. Dashed black lines indicate FI of the isotype control Ab in shGBPp1 cells or shSpectrin2 cells. $*p < 0.05$, $**p < 0.01$, $***p < 0.005$.

GBP-1–silenced T cells. We assessed the spreading of GBP-1–silenced Jurkat T cells on a surface coated with OKT3. GBP-1–silenced cells showed a more pronounced spreading on the CD3 surface than control cells (Fig. 5A). Interestingly, the difference in spreading was less outspoken on a surface cocoated with CD3 and CD28 mAbs (Fig. 5A–C, Supplemental Fig. 3, Supplemental Movies 1–4).

Besides β-actin and plastin-2, we identified by mass spectrometry three other GBP-1 interacting proteins (Fig. 3D) that interfere with the cytoskeleton and early TCR signaling: stomatin-like protein 2 (STOML2) (32, 33), myosin regulatory L chain MRCL3 variant (MRCL3) (34), and the βII-spectrin. βII-Spectrin was described to be involved in CD3 and CD45 surface display and IL-2 production (35, 36). We found that CD45 and CD3 surface expression was enhanced in GBP-1–silenced Jurkat T cells, whereas the levels of several other surface receptors such as CD11a, CD18, and CD43 were not altered (Fig. 5D). We confirmed the higher surface expression of CD45 and CD3 upon silencing of

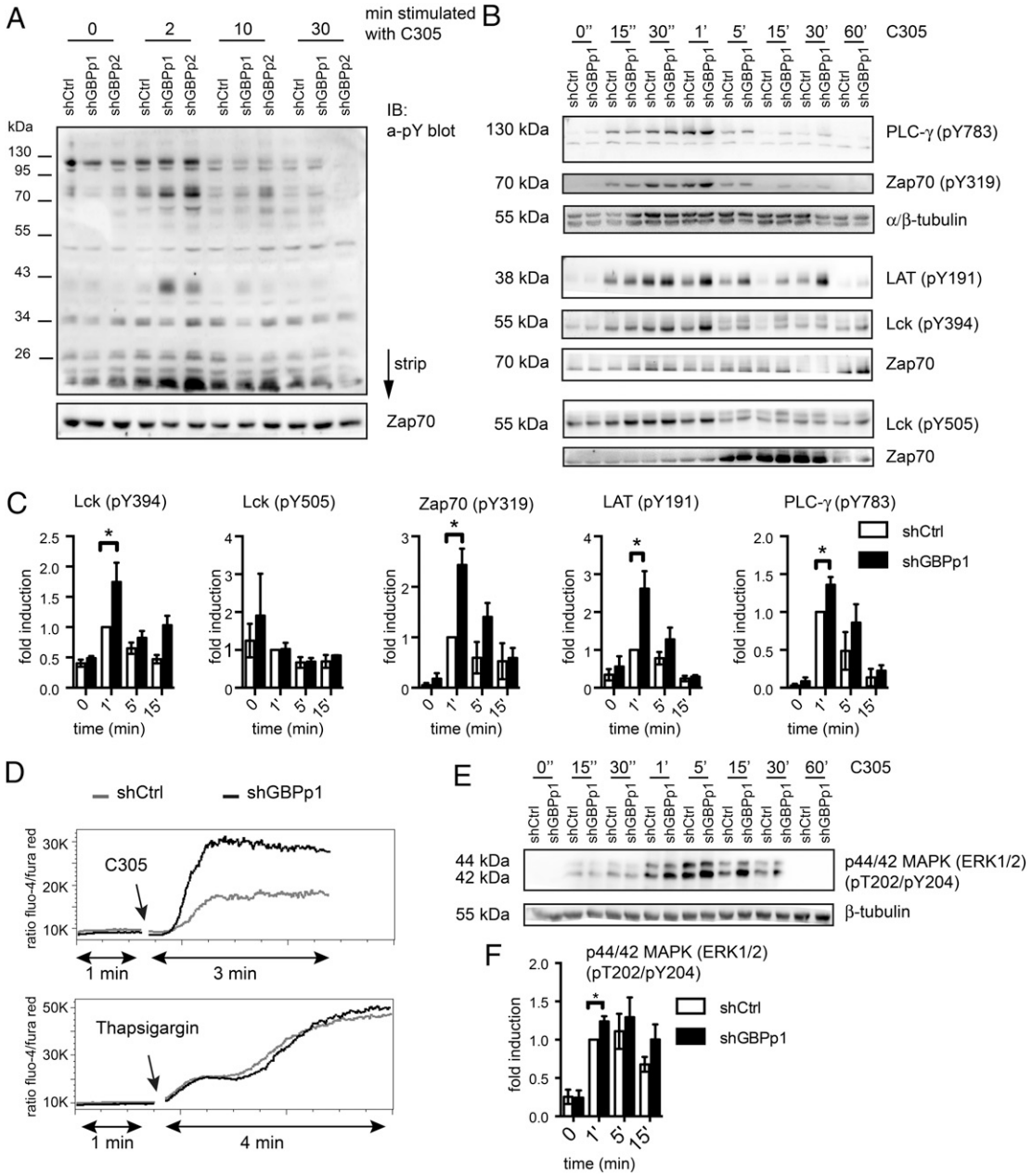

FIGURE 6. Hyperphosphorylation of TCR signaling molecules in GBP-1–silenced Jurkat T cells. (**A**) Anti-phosphotyrosine mAb–stained blots of GBP-1–silenced or control silenced Jurkat T cells stimulated with the TCR mAb C305 for the indicated time points. *Pan*-Zap70 staining acted as loading control. (**B**) Phosphotyrosine blots of Lck, LAT, Zap70, and PLC-γ of lysates of GBP-1–silenced or control silenced Jurkat T cells. The cells were stimulated with TCR mAb C305 for the shown time points. α/β-Tubulin acted as loading control for phospho-Zap70 and phospho–PLC-γ, and pan-Zap70 acted as loading control for phospho-LAT and phospho-Lck. (**C**) Densitometric evaluations of the indicated signaling molecules. The phospho-specific Ab signals were normalized to their corresponding loading control. The value obtained for the control silenced Jurkat T cells after 1 min of stimulation was set to 1, and all other values refer to that value. (**D**) Intracellular Ca^{2+} flux of GBP-1 or control silenced Jurkat T cells stimulated with either the TCR mAb C305 (*upper panel*) or with 1 μM thapsigargin (*lower panel*). (**E**) Phosphoblot of the MAPK ERK of GBP-1 or control silenced cells stimulated for the indicated time points. Tubulin acted as loading control. (**F**) Densitometric evaluation of ERK phosphorylation. (A, B, D, and E) One representative experiment of at least three is shown. (C and F) Bars represent the mean; error bars represent SD of at least three independent experiments. $*p < 0.05$.

GBP-1 in primary T lymphocytes (Fig. 5E). Thus, these results suggest that the interaction of GBP-1 with βII-spectrin altered CD3 and CD45 surface expression. To test whether βII-spectrin is involved in the GBP-1–mediated negative regulation of TCR signaling, we cosilenced βII-spectrin and GBP-1 in Jurkat T cells. We used two different shRNA constructs for βII-spectrin silencing, which lead to either 20% (shSpectrin1) or 95% silencing (shSpectrin2; Fig. 5H). Silencing of βII-spectrin by both shRNA constructs evoked decreased expression of CD3 and CD45 in Jurkat T cells (Fig. 5I, 5J). Experiments in Jurkat T cells expressing an IL-2 luciferase reporter construct and stimulated with SEE-pulsed Raji B cells showed that silencing of βII-spectrin decreased IL-2 expression. Moreover, the overshooting expression of IL-2 in GBP-1–silenced cells was partially reversed by cosilencing of βII-spectrin (Fig. 5K).

GBP-1 interferes with early TCR signaling

The alterations in CD3 and CD45 expression, and cytoskeletal modifications found in GBP-1–silenced cells might influence T cell signaling. Therefore, we probed with an anti-phosphotyrosine mAb lysates of GBP-1–silenced and control silenced Jurkat T cells stimulated with the TCR β-chain mAb C305 for up to 30 min. With both shRNA constructs used for GBP-1 silencing, we observed higher tyrosine phosphorylation of several signaling molecules compared with the control cells (Fig. 6A). To investigate this finding in more detail, we used phosphorylation-site–specific Abs against important signaling molecules and stimulated over a broader time range (Fig. 6B, Supplemental Fig. 4). Lck was consistently higher phosphorylated at the activatory position 394 in GBP-1–silenced Jurkat T cells, whereas the inhibitory tyrosine residue at position 505 was not affected (Fig. 6C). All subsequent TCR signaling molecules tested showed higher phosphorylation in GBP-1–silenced cells (Fig. 6B, 6C, Supplemental Fig. 4). To see whether the differences in early TCR signaling were transferred to distal parts of the signaling cascade, we monitored intracellular Ca^{2+} concentrations by flow cytometry. GBP-1–silenced cells stimulated via cross-linking of the TCR exhibited elevated intracellular Ca^{2+} levels. When we used the sarcoplasmic/endoplasmic reticulum calcium ATPase inhibitor, thapsigargin, thereby bypassing early TCR signaling, the difference in the intracellular Ca^{2+} concentration between GBP-1–silenced and control silenced cells disappeared (Fig. 6D). We also detected higher phosphorylation of ERK in GBP-1–silenced Jurkat T cells, proving also higher activation of distal signaling proteins (Fig. 6E, 6F, Supplemental Fig. 4).

Finally, we wanted to corroborate the earlier findings in primary T lymphocytes isolated from human peripheral blood. We observed higher phosphorylation of PLC-γ (Fig. 7A, 7B) and higher intracellular Ca^{2+} concentration upon cross-linking of CD3 (Fig. 7C) in GBP-1–silenced T lymphocytes. Furthermore, LAT was higher phosphorylated in the GBP-1–silenced T lymphocytes. Higher phosphorylation of the MAPK ERK indicated that in GBP-1–silenced primary T lymphocytes, the higher activation of early TCR signaling molecules was transduced to late signaling events, confirming our findings with Jurkat T cells (Fig. 7A, 7B).

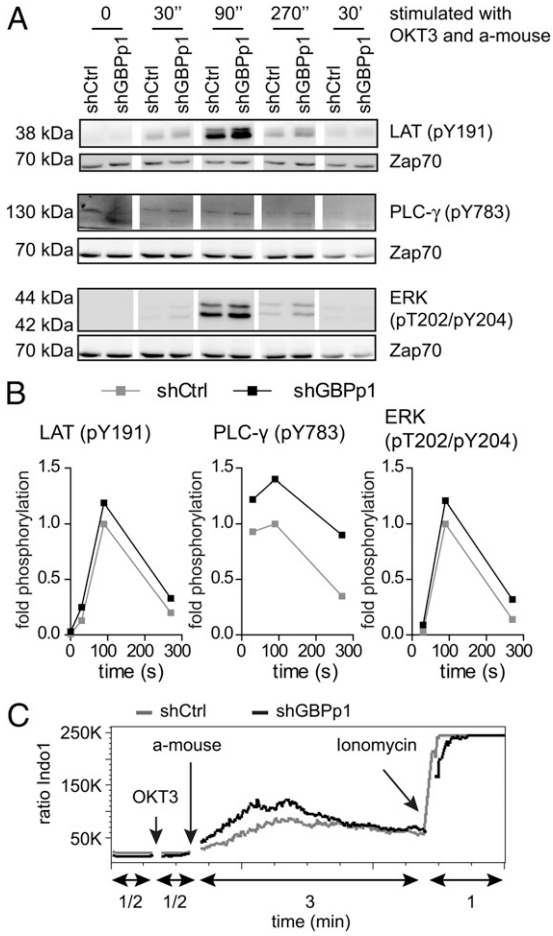

FIGURE 7. Hyperphosphorylation of TCR signaling molecules in GBP-1–silenced primary human T lymphocytes. (**A**) Phosphorylation specific blots of LAT, PLC-γ, and ERK of lysates of GBP-1 or control silenced primary T lymphocytes upon cross-linking CD3 mAb OKT3 for the indicated periods. *Pan*-Zap70 acted as loading control. One representative blot of at least three independent experiments is shown. (**B**) Densitometric evaluation of the signaling molecules in the Western blot of (A). The phosphospecific Ab signals were normalized to their corresponding loading control, and the value obtained for control silenced T cells after 90 s of stimulation was set to 1. All other values refer to that value. (**C**) Flow cytometric analysis of intracellular Ca^{2+} flux of GBP-1–silenced or control silenced primary T lymphocytes upon cross-linking with CD3 mAb OKT3. At the end of the assay, 1 μM ionomycin was added to prove equal loading of the cells with the Ca^{2+}-sensing dye Indo-1. One representative experiment of three is shown.

Discussion

Screening of human cells and tissues showed that GBP-1 expression is highest in T lymphocytes (16). We show in this article that this basal expression of GBP-1 can be further increased by stimulation via the TCR. Most likely this is due to the fact that T cells produce IFN-γ upon stimulation that leads to subsequent activation of the GBP-1 promoter (37, 38). Recently, an alternative pathway of promoter activation of GBP-1 was described involving Src and p38 kinases (39). Thus, it is also possible that TCR activation directly influences GBP-1 expression. We detected the highest expression of GBP-1 24 h after onset of T cell stimulation, a typical time point when negative regulators are getting expressed (40). Therefore, this finding was our first hint that GBP-1 may assist in tuning down T cell responses.

The data presented in this article establish GBP-1 as a negative regulator of T cell activation by interfering with early TCR signaling. Early TCR signaling molecules are hyperphosphorylated in GBP-1–silenced cells. Moreover, treatment of T cells with agents bypassing early signaling events do not show any difference between GBP-1–silenced and control silenced T cells: specifically, IL-2 promoter activity was not changed upon stimulation of T cells using the PKC activator PMA plus the Ca^{2+} ionophore ionomycin or by evoking a Ca^{2+} response with the sarcoplasmic/endoplasmic reticulum calcium ATPase inhibitor thapsigargin.

To get an insight into the molecular mechanism of GBP-1 in cells in general and in T cells in particular, we screened for interaction partners using mass spectrometry. Currently, little is known about cellular partners of GBP-1. It is known that GBP-1 binds (besides homodimerization and heterodimerization with GBP family members) (41, 42) to the cytoskeletal proteins β-IIITubulin and PIM1 (14). Five among the 10 potential GBP-1 binding partners identified by us by mass spectrometry (multisynthetase complex auxiliary component p43, plastin-2, STOML2, MRCL3, and βII-spectrin) are described to be involved in the remodeling of the (actin-) cytoskeleton (33, 36, 43, 44) and 4 of these 5 (plastin-2, STOML2, MRCL3, and βII-spectrin) to influence T cell activation (30, 32–36, 44–46). Based on the fact that IL-2 expression is abrogated in plastin-2 knockout mice, we suspected plastin-2 to be involved in the GBP-1–mediated IL-2 regulation. However, we could not confirm the results obtained in mice with human T cells. We found that plastin-2 silencing neither blunted the higher IL-2 expression observed in GBP-1–silenced cells nor decreased IL-2 expression on its own, pointing to a plastin-2–independent effect of GBP-1 on human IL-2 regulation and to a different function of plastin-2 in mouse versus human T cells. This finding was at first glance hard to understand, because our pull-down and SILAC mass spectrometry experiments further showed that GBP-1 regulated the phosphorylation status of plastin-2 at Ser^5, which was shown to increase its actin-bundling activity (29, 47), and moreover, GBP-1 itself bound to β-actin (Fig. 4A–C). Strikingly, we found that this physical and functional interaction of GBP-1 with plastin-2 regulates CD69 surface expression (Fig. 4E). Finally, double-silencing experiments identified βII-spectrin as one of the molecular cooperation partners of GBP-1 regulating IL-2 activation.

It was described that the βII-spectrin cytoskeleton influences IL-2 production in T cells by mediating CD3 and CD45 surface expression (35, 36). We show in this article that GBP-1 interferes with CD3 and CD45 surface display (Fig. 5D–G). Thus, we speculated that the interaction of GBP-1 with actin and βII-spectrin would control the mobility and compartmentalization of TCR/CD3 and its signaling molecules. Higher TCR/CD3 expression on the cell surface makes more triggering molecules for Ag and more cytoplasmic binding sites (ITAMs) for juxtamembrane signaling molecules available. Higher CD45 expression should lead to lower phosphorylation at the inhibitory tyrosine residue 505 of Lck, and thus higher activity of this central kinase of TCR/CD3 signaling. In this respect, it is at first glance a paradox that Lck is not lower phosphorylated at the inhibitory tyrosine position 505 in GBP-1–silenced cells. Indeed, it has been reported that low expression levels of CD45 lead to hypoactivation, and small changes in CD45 expression have a big effect in T cell activation (48). However, Lck is higher phosphorylated at the activatory tyrosine position 394, and more important, the ratio of phosphorylation at 394 to 505 is higher in GBP-1–silenced cells. Thus, we speculate that GBP-1, via changing expression of CD45 and CD3 through interaction with βII-spectrin, shifts the balance of inactivated Lck-pools, which are either unphosphorylated on both the activatory tyrosine 394 and the inhibitory tyrosine 505 or phosphorylated on tyrosine 505 only, to the activated Lck pools, which are either phosphorylated on tyrosine 394 or on both tyrosine residues (49, 50). Nonetheless, nearly complete βII-spectrin silencing did not completely blunt the overshooting IL-2 expression in GBP-1–silenced T cells, which indicates involvement of additional proteins and processes in the GBP-1–mediated effect on TCR signaling.

In summary, we established the IFN-γ–inducible GBP-1 as a new negative regulator of early TCR signaling. We identified previously unknown cellular binding partners of GBP-1, which together with GBP-1 modify T cell activation. However, some of the newly identified binding partners of GBP-1 could also provide, apart from T cell stimulation, an explanation for the molecular basis of the diverse physiological functions of GBP-1 described so far. Because most of these proteins regulate cytoskeletal processes, we suggest that T cells can regulate via IFN-γ cytoskeleton-dependent cellular functions at several levels in an autocrine and paracrine manner through GBP-1.

Acknowledgments

We thank Eva Steinhuber and Margarethe Merio for excellent technical assistance. We are grateful to the imaging core facility of the Medical University of Vienna.

Disclosures

The authors have no financial conflicts of interest.

References

1. MacMicking, J. D. 2004. IFN-inducible GTPases and immunity to intracellular pathogens. *Trends Immunol.* 25: 601–609.
2. Lubeseder-Martellato, C., E. Guenzi, A. Jörg, K. Töpolt, E. Naschberger, E. Kremmer, C. Zietz, E. Tschachler, P. Hutzler, M. Schwemmle, et al. 2002. Guanylate-binding protein-1 expression is selectively induced by inflammatory cytokines and is an activation marker of endothelial cells during inflammatory diseases. *Am. J. Pathol.* 161: 1749–1759.
3. Naschberger, E., T. Werner, A. B. Vicente, E. Guenzi, K. Töpolt, R. Leubert, C. Lubeseder-Martellato, P. J. Nelson, and M. Stürzl. 2004. Nuclear factor-kappaB motif and interferon-alpha-stimulated response element co-operate in the activation of guanylate-binding protein-1 expression by inflammatory cytokines in endothelial cells. *Biochem. J.* 379: 409–420.
4. Guenzi, E., K. Töpolt, E. Cornali, C. Lubeseder-Martellato, A. Jörg, K. Matzen, C. Zietz, E. Kremmer, F. Nappi, M. Schwemmle, et al. 2001. The helical domain of GBP-1 mediates the inhibition of endothelial cell proliferation by inflammatory cytokines. *EMBO J.* 20: 5568–5577.
5. Syguda, A., M. Bauer, U. Benscheid, N. Ostler, E. Naschberger, S. Ince, M. Stürzl, and C. Herrmann. 2012. Tetramerization of human guanylate-binding protein 1 is mediated by coiled-coil formation of the C-terminal α-helices. *FEBS J.* 279: 2544–2554.
6. Prakash, B., L. Renault, G. J. Praefcke, C. Herrmann, and A. Wittinghofer. 2000. Triphosphate structure of guanylate-binding protein 1 and implications for nucleotide binding and GTPase mechanism. *EMBO J.* 19: 4555–4564.
7. Prakash, B., G. J. Praefcke, L. Renault, A. Wittinghofer, and C. Herrmann. 2000. Structure of human guanylate-binding protein 1 representing a unique class of GTP-binding proteins. *Nature* 403: 567–571.
8. Guenzi, E., K. Töpolt, C. Lubeseder-Martellato, A. Jörg, E. Naschberger, R. Benelli, A. Albini, and M. Stürzl. 2003. The guanylate binding protein-1 GTPase controls the invasive and angiogenic capability of endothelial cells through inhibition of MMP-1 expression. *EMBO J.* 22: 3772–3782.
9. Weinländer, K., E. Naschberger, M. H. Lehmann, P. Tripal, W. Paster, H. Stockinger, C. Hohenadl, and M. Stürzl. 2008. Guanylate binding protein-1 inhibits spreading and migration of endothelial cells through induction of integrin alpha4 expression. *FASEB J.* 22: 4168–4178.
10. MacMicking, J. D. 2012. Interferon-inducible effector mechanisms in cell-autonomous immunity. *Nat. Rev. Immunol.* 12: 367–382.
11. Kim, B. H., A. R. Shenoy, P. Kumar, R. Das, S. Tiwari, and J. D. MacMicking. 2011. A family of IFN-γ-inducible 65-kD GTPases protects against bacterial infection. *Science* 332: 717–721.
12. Anderson, S. L., J. M. Carton, J. Lou, L. Xing, and B. Y. Rubin. 1999. Interferon-induced guanylate binding protein-1 (GBP-1) mediates an antiviral effect against vesicular stomatitis virus and encephalomyocarditis virus. *Virology* 256: 8–14.
13. Itsui, Y., N. Sakamoto, S. Kakinuma, M. Nakagawa, Y. Sekine-Osajima, M. Tasaka-Fujita, Y. Nishimura-Sakurai, G. Suda, Y. Karakama, K. Mishima, et al. 2009. Antiviral effects of the interferon-induced protein guanylate binding protein 1 and its interaction with the hepatitis C virus NS5B protein. *Hepatology* 50: 1727–1737.
14. De Donato, M., M. Mariani, L. Petrella, E. Martinelli, G. F. Zannoni, V. Vellone, G. Ferrandina, S. Shahabi, G. Scambia, and C. Ferlini. 2012. Class III β-tubulin and the cytoskeletal gateway for drug resistance in ovarian cancer. *J. Cell. Physiol.* 227: 1034–1041.
15. Duan, Z., R. Foster, K. A. Brakora, R. Z. Yusuf, and M. V. Seiden. 2006. GBP1 overexpression is associated with a paclitaxel resistance phenotype. *Cancer Chemother. Pharmacol.* 57: 25–33.
16. Su, A. I., T. Wiltshire, S. Batalov, H. Lapp, K. A. Ching, D. Block, J. Zhang, R. Soden, M. Hayakawa, G. Kreiman, et al. 2004. A gene atlas of the mouse and human protein-encoding transcriptomes. *Proc. Natl. Acad. Sci. USA* 101: 6062–6067.
17. Feng, C. G., L. Zheng, D. Jankovic, A. Báfica, J. L. Cannons, W. T. Watford, D. Chaussabel, S. Hieny, P. Caspar, P. L. Schwartzberg, et al. 2008. The immunity-related GTPase Irgm1 promotes the expansion of activated CD4+ T cell populations by preventing interferon-gamma-induced cell death. *Nat. Immunol.* 9: 1279–1287.

18. Singh, S. B., A. S. Davis, G. A. Taylor, and V. Deretic. 2006. Human IRGM induces autophagy to eliminate intracellular mycobacteria. *Science* 313: 1438–1441.
19. Bekpen, C., J. P. Hunn, C. Rohde, I. Parvanova, L. Guethlein, D. M. Dunn, E. Glowalla, M. Leptin, and J. C. Howard. 2005. The interferon-inducible p47 (IRG) GTPases in vertebrates: loss of the cell autonomous resistance mechanism in the human lineage. *Genome Biol.* 6: R92.
20. Cox, B., and A. Emili. 2006. Tissue subcellular fractionation and protein extraction for use in mass-spectrometry-based proteomics. *Nat. Protoc.* 1: 1872–1878.
21. Muhammad, A., H. B. Schiller, F. Forster, P. Eckerstorfer, R. Geyeregger, V. Leksa, G. J. Zlabinger, M. Sibilia, A. Sonnleitner, W. Paster, and H. Stockinger. 2009. Sequential cooperation of CD2 and CD48 in the buildup of the early TCR signalosome. *J. Immunol.* 182: 7672–7680.
22. Wiśniewski, J. R., A. Zougman, N. Nagaraj, and M. Mann. 2009. Universal sample preparation method for proteome analysis. *Nat. Methods* 6: 359–362.
23. Sharma, K., R. M. Vabulas, B. Macek, S. Pinkert, J. Cox, M. Mann, and F. U. Hartl. 2012. Quantitative proteomics reveals that Hsp90 inhibition preferentially targets kinases and the DNA damage response. *Mol. Cell. Proteomics* 11: M111.014654.
24. Cox, J., and M. Mann. 2008. MaxQuant enables high peptide identification rates, individualized p.p.b.-range mass accuracies and proteome-wide protein quantification. *Nat. Biotechnol.* 26: 1367–1372.
25. Cox, J., N. Neuhauser, A. Michalski, R. A. Scheltema, J. V. Olsen, and M. Mann. 2011. Andromeda: a peptide search engine integrated into the MaxQuant environment. *J. Proteome Res.* 10: 1794–1805.
26. Luber, C. A., J. Cox, H. Lauterbach, B. Fancke, M. Selbach, J. Tschopp, S. Akira, M. Wiegand, H. Hochrein, M. O'Keeffe, and M. Mann. 2010. Quantitative proteomics reveals subset-specific viral recognition in dendritic cells. *Immunity* 32: 279–289.
27. Hesse, J., M. Sonnleitner, A. Sonnleitner, G. Freudenthaler, J. Jacak, O. Höglinger, H. Schindler, and G. J. Schütz. 2004. Single-molecule reader for high-throughput bioanalysis. *Anal. Chem.* 76: 5960–5964.
28. Bailey, S., and P. J. Macardle. 2006. A flow cytometric comparison of Indo-1 to fluo-3 and Fura Red excited with low power lasers for detecting Ca(2+) flux. *J. Immunol. Methods* 311: 220–225.
29. Janji, B., A. Giganti, V. De Corte, M. Catillon, E. Bruyneel, D. Lentz, J. Plastino, J. Gettemans, and E. Friederich. 2006. Phosphorylation on Ser5 increases the F-actin-binding activity of L-plastin and promotes its targeting to sites of actin assembly in cells. *J. Cell Sci.* 119: 1947–1960.
30. Wabnitz, G. H., T. Köcher, P. Lohneis, C. Stober, M. H. Konstandin, B. Funk, U. Sester, M. Wilm, M. Klemke, and Y. Samstag. 2007. Costimulation induced phosphorylation of L-plastin facilitates surface transport of the T cell activation molecules CD69 and CD25. *Eur. J. Immunol.* 37: 649–662.
31. Bunnell, S. C., V. Kapoor, R. P. Trible, W. Zhang, and L. E. Samelson. 2001. Dynamic actin polymerization drives T cell receptor-induced spreading: a role for the signal transduction adaptor LAT. *Immunity* 14: 315–329.
32. Christie, D. A., M. G. Kirchhof, S. Vardhana, M. L. Dustin, and J. Madrenas. 2012. Mitochondrial and plasma membrane pools of stomatin-like protein 2 coalesce at the immunological synapse during T cell activation. *PLoS ONE* 7: e37144.
33. Kirchhof, M. G., L. A. Chau, C. D. Lemke, S. Vardhana, P. J. Darlington, M. E. Márquez, R. Taylor, K. Rizkalla, I. Blanca, M. L. Dustin, and J. Madrenas. 2008. Modulation of T cell activation by stomatin-like protein 2. *J. Immunol.* 181: 1927–1936.
34. Ilani, T., G. Vasiliver-Shamis, S. Vardhana, A. Bretscher, and M. L. Dustin. 2009. T cell antigen receptor signaling and immunological synapse stability require myosin IIA. *Nat. Immunol.* 10: 531–539.
35. Cairo, C. W., R. Das, A. Albohy, Q. J. Baca, D. Pradhan, J. S. Morrow, D. Coombs, and D. E. Golan. 2010. Dynamic regulation of CD45 lateral mobility by the spectrin-ankyrin cytoskeleton of T cells. *J. Biol. Chem.* 285: 11392–11401.
36. Pradhan, D., and J. Morrow. 2002. The spectrin-ankyrin skeleton controls CD45 surface display and interleukin-2 production. *Immunity* 17: 303–315.
37. Olszewski, M. A., J. Gray, and D. J. Vestal. 2006. In silico genomic analysis of the human and murine guanylate-binding protein (GBP) gene clusters. *J. Interferon Cytokine Res.* 26: 328–352.
38. Decker, T., D. J. Lew, and J. E. Darnell, Jr. 1991. Two distinct alpha-interferon-dependent signal transduction pathways may contribute to activation of transcription of the guanylate-binding protein gene. *Mol. Cell. Biol.* 11: 5147–5153.
39. Li, M., A. Mukasa, M. M. Inda, J. Zhang, L. Chin, W. Cavenee, and F. Furnari. 2011. Guanylate binding protein 1 is a novel effector of EGFR-driven invasion in glioblastoma. *J. Exp. Med.* 208: 2657–2673.
40. Pentcheva-Hoang, T., E. Corse, and J. P. Allison. 2009. Negative regulators of T-cell activation: potential targets for therapeutic intervention in cancer, autoimmune disease, and persistent infections. *Immunol. Rev.* 229: 67–87.
41. Britzen-Laurent, N., M. Bauer, V. Berton, N. Fischer, A. Syguda, S. Reipschläger, E. Naschberger, C. Herrmann, and M. Stürzl. 2010. Intracellular trafficking of guanylate-binding proteins is regulated by heterodimerization in a hierarchical manner. *PLoS ONE* 5: e14246.
42. Ghosh, A., G. J. Praefcke, L. Renault, A. Wittinghofer, and C. Herrmann. 2006. How guanylate-binding proteins achieve assembly-stimulated processive cleavage of GTP to GMP. *Nature* 440: 101–104.
43. Jackson, V. C., S. Dewilde, A. G. Albo, K. Lis, D. Corpillo, and B. Canepa. 2011. The activity of aminoacyl-tRNA synthetase-interacting multi-functional protein 1 (AIMP1) on endothelial cells is mediated by the assembly of a cytoskeletal protein complex. *J. Cell. Biochem.* 112: 1857–1868.
44. Wabnitz, G. H., P. Lohneis, H. Kirchgessner, B. Jahraus, S. Gottwald, M. Konstandin, M. Klemke, and Y. Samstag. 2010. Sustained LFA-1 cluster formation in the immune synapse requires the combined activities of L-plastin and calmodulin. *Eur. J. Immunol.* 40: 2437–2449.
45. Wang, C., S. C. Morley, D. Donermeyer, I. Peng, W. P. Lee, J. Devoss, D. M. Danilenko, Z. Lin, J. Zhang, J. Zhou, et al. 2010. Actin-bundling protein L-plastin regulates T cell activation. *J. Immunol.* 185: 7487–7497.
46. Iida, N., V. B. Lokeshwar, and L. Y. Bourguignon. 1994. Mapping the fodrin binding domain in CD45, a leukocyte membrane-associated tyrosine phosphatase. *J. Biol. Chem.* 269: 28576–28583.
47. Al Tanoury, Z., E. Schaffner-Reckinger, A. Halavatyi, C. Hoffmann, M. Moes, E. Hadzic, M. Catillon, M. Yatskou, and E. Friederich. 2010. Quantitative kinetic study of the actin-bundling protein L-plastin and of its impact on actin turn-over. *PLoS ONE* 5: e9210.
48. McNeill, L., R. J. Salmond, J. C. Cooper, C. K. Carret, R. L. Cassady-Cain, M. Roche-Molina, P. Tandon, N. Holmes, and D. R. Alexander. 2007. The differential regulation of Lck kinase phosphorylation sites by CD45 is critical for T cell receptor signaling responses. *Immunity* 27: 425–437.
49. Paster, W., C. Paar, P. Eckerstorfer, A. Jakober, K. Drbal, G. J. Schütz, A. Sonnleitner, and H. Stockinger. 2009. Genetically encoded Förster resonance energy transfer sensors for the conformation of the Src family kinase Lck. *J. Immunol.* 182: 2160–2167.
50. Nika, K., C. Soldani, M. Salek, W. Paster, A. Gray, R. Etzensperger, L. Fugger, P. Polzella, V. Cerundolo, O. Dushek, et al. 2010. Constitutively active Lck kinase in T cells drives antigen receptor signal transduction. *Immunity* 32: 766–777.
51. Boulon, S., Y. Ahmad, L. Trinkle-Mulcahy, C. Verheggen, A. Cobley, P. Gregor, E. Bertrand, M. Whitehorn, and A. I. Lamond. 2010. Establishment of a protein frequency library and its application in the reliable identification of specific protein interaction partners. *Mol. Cell. Proteomics* 9: 861–879.

Supplementary Figure 1

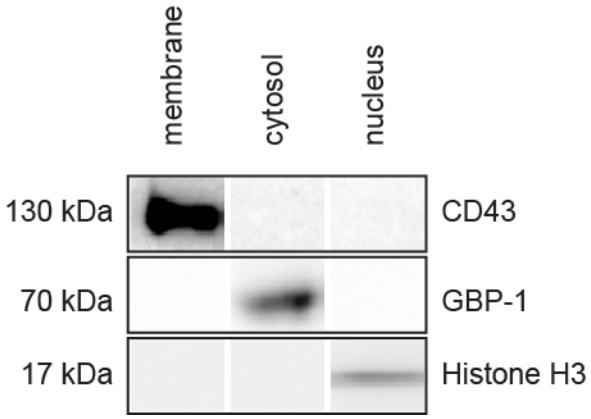

Supplementary Figure 1:
GBP-1 is exclusively expressed in the cytosolic fraction of Jurkat T cells. Immunoblotting analysis of membrane, cytosolic and nuclear fractions of Jurkat T cells. CD43 and histone H3.1 were used as markers for the membrane and nuclear fraction, respectively.

Supplementary Figure 2

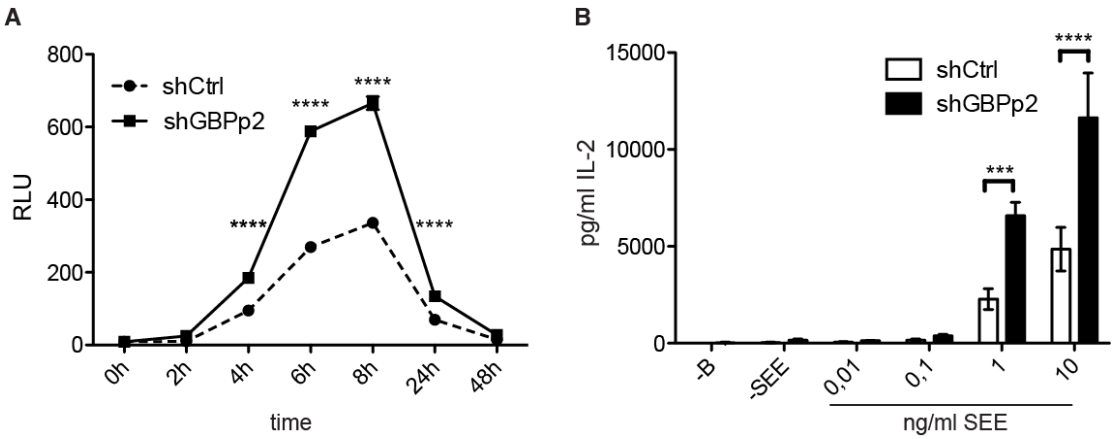

Supplementary Figure 2:
Higher IL-2 expression in GBP-1 silenced Jurkat T cells is independent of duration of stimulation and strength of the stimulus. **A** RLUs of GBP-1 and control silenced Jurkat T cells stimulated for different time points with Raji B cells pulsed with 10 ng/ml SEE. **B** IL-2 concentration in the supernatants of GBP-1 silenced and control-silenced Jurkat T cells stimulated with Raji B cells pulsed with the indicated concentrations of SEE. Shown are mean values. Error bars represent SD.

Supplementary Figure 3

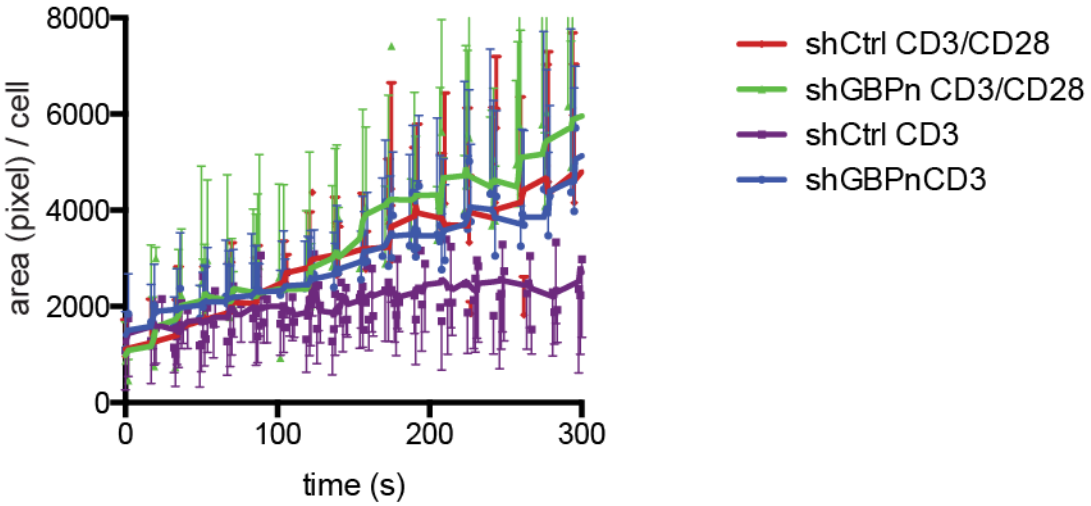

Supplementary Figure 3:
Statistic evaluation of the spreading area over time of individual Jurkat T cells on surfaces coated with the indicated antibodies. The following numbers of cells were evaluated: shGBP-1 on the OKT3 surface: n = 58, shCtrl on the OKT3 surface: n = 60, shGBP-1 on the OKT3/Leu28 surface: n = 29 and shCtrl on the OKT3/Leu28 surface: n = 32. The mean cell area in pixels is shown per time point. Error bars represent SD.

Supplementary Figure 4

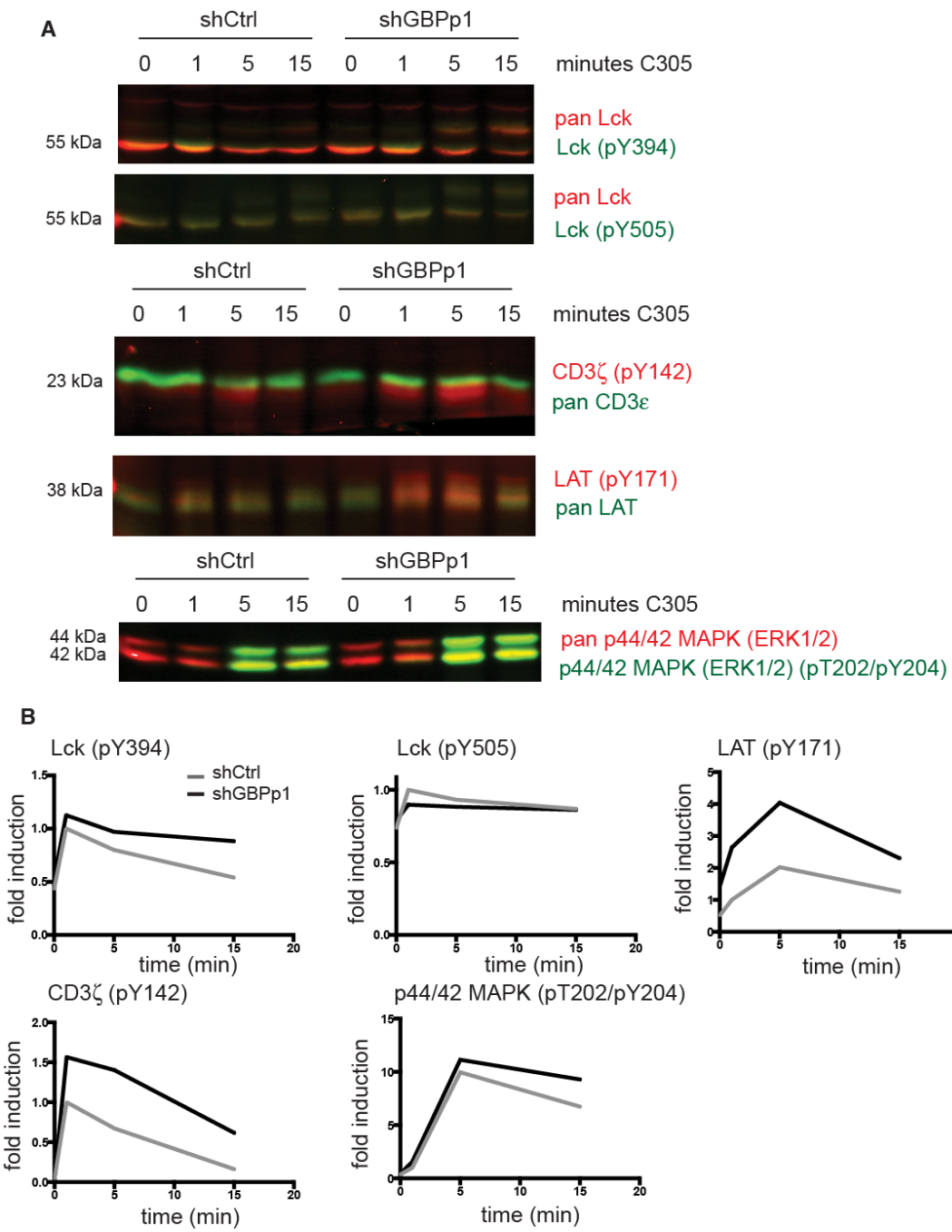

Supplementary Figure 4:
Higher phosphorylation status of TCR signaling molecules in GBP-1 silenced Jurkat T cells. **A** Phosphotyrosine blots of Lck, CD3, LAT and erk of lysates of control and GBP-1 silenced Jurkat T cells. The cells were stimulated with the anti-TCR mAb C305 for the indicated time points. Corresponding total protein amounts acted as loading controls. Images were obtained using the Licor imaging system and fluorescently labeled Abs. **B** Densitometric evaluations of the indicated molecules of the blots in A. The phospho specific Ab signals were normalized to the corresponding total protein. The value obtained for the control silenced Jurkat cells after 1 min of stimulation was set to 1 and all other values refer to that value.

Supplementary video 1:

Spreading of Jurkat T cells transduced with a control shRNA on an OKT3 coated surface.

Supplementary video 2:

Spreading of Jurkat T cells transduced with the GBPp1 shRNA on an OKT3 coated surface.

Supplementary video 3:

Spreading of Jurkat T cells transduced with a control shRNA on an OKT3 and Leu28 coated surface.

Supplementary video 4:

Spreading of Jurkat T cells transduced with the GBPp1 shRNA on an OKT3 and Leu28 coated surface.